Radiometric validation of NASA's Ames Research Center's Sensor Calibration Laboratory

Steven W. Brown, B. Carol Johnson, Stuart F. Biggar, Edward F. Zalewski, John Cooper, Pavel Hajek, Edward Hildum, Patrick Grant, Robert A. Barnes, and James J. Butler

The National Aeronautics and Space Administration's (NASA's) Ames Research Center's Airborne Sensor Facility (ASF) is responsible for the calibration of several airborne Earth-viewing sensor systems in support of NASA Earth Observing System (EOS) investigations. The primary artifact used to calibrate these sensors in the reflective solar region from 400 to 2500 nm is a lamp-illuminated integrating sphere source. In September 1999, a measurement comparison was made at the Ames ASF Sensor Calibration Facility to validate the radiometric scale, establish the uncertainties assigned to the radiance of this source, and examine its day-to-day repeatability. The comparison was one of a series of validation activities overseen by the EOS Calibration Program to ensure the radiometric calibration accuracy of sensors used in long-term, global, remote-sensing studies. Results of the comparison, including an evaluation of the Ames Sensor Calibration Laboratory (SCL) measurement procedures and assigned radiometric uncertainties, provide a validation of their radiometric scale at the time of the comparison. Additionally, the maintenance of the radiance scale was evaluated by use of independent, long-term, multiyear radiance validation measurements of the Ames sphere source. This series of measurements provided an independent assessment of the radiance values assigned to integrating sphere sources by the Ames SCF. Together, the measurements validate the SCF radiometric scale and assigned uncertainties over the time period from September 1999 through July 2003.

OCIS codes: 120.0120, 120.3940, 120.4800, 120.5410, 120.5630, 120.5700.

1. Introduction

The NASA Ames Research Center's Sensor Calibration Laboratory (SCL) is responsible for radiometric calibrations of the Earth Observing System (EOS) airborne remote-sensing instruments from the visible through the thermal infrared, i.e., from 350 nm to 15 μm. Several instruments, including the Moderate Resolution Imaging Spectroradiometer (MODIS) Airborne Simulator (MAS) and the Advanced Spaceborne Thermal Emission and Reflection Radiometer (ASTER) airborne simulator, operate in the 450 nm–2.5 μm spectral region. The MAS and the MODIS ASTER (MASTER) instruments support the design, development, and testing of MODIS and ASTER algorithms and, with careful calibration, can provide a vicarious (on-orbit) calibration for those instruments.[1,2] For proper test and evaluation of algorithms designed to calculate the top of the atmosphere radiance, it is important that the responsivities of the airborne instrumentation be known and the radiometric uncertainties and sources of error be identified and understood. Ideally, in vicarious calibration applications, the radiometric uncertainties in MAS and MASTER airborne remote-sensing measurements should be commensurate with the requirements for the MODIS and the ASTER.

Aircraft remote-sensing instruments are calibrated over the spectral range 350–2500 nm on a prefield and a postfield deployment basis in the laboratory at NASA's Ames SCL by use of a 76 cm diameter, lamp-illuminated barium-sulfate-coated integrating sphere source (ISS) with a known spectral radiance. The sphere is oriented

S. W. Brown and B. C. Johnson are with the National Institute of Standards and Technology, Gaithersburg, Maryland 20899. S. F. Biggar and E. F. Zalewski are with the University of Arizona's Remote Sensing Group, Tucson, Arizona 85721. J. Cooper is with the Science Systems Applications, Inc., Lanham, Maryland 20706. P. Hajek, E. Hildum, and P. Grant are with Science Applications International Corporation, Moffet Field, California 94035. R. A. Barnes (rbarnes@seawifs.gsfc.nasa.gov) is with Science Applications International Corporation, Beltsville, Maryland 20705. J. J. Butler is with NASA's Goddard Space Flight Center, Greenbelt, Maryland 20771.

Received 2 November 2004; revised manuscript received 13 April 2005; accepted 27 June 2005.

0003-6935/05/306426-18$15.00/0

such that the exit port is upward looking, illuminating the airborne instruments in the same orientation as during their in-flight operation. Relative changes in the airborne instruments are monitored in the field by use of a 50 cm diameter integrating hemisphere and other sphere sources.[3]

The 76 cm ISS is maintained, monitored, and calibrated at the Ames SCL on a periodic basis. The Ames sphere calibration methodology is based on the transfer of a radiance scale obtained from a reflectance panel (or plaque) and a an irradiance standard lamp calibrated to the ISS. An Analytical Spectral Devices (ASD) FieldSpec radiometer[4] is used to transfer the radiance scale from the reflectance plaque to the integrating sphere. Target combined standard uncertainties in the sphere radiance are 3% in the visible and 6% in the shortwave infrared. To validate the measurement protocol and assist in establishing the uncertainties in the radiometric calibration of the integrating sphere, measurement comparisons of the ISS radiance were periodically conducted among the Ames transfer standard radiometer, the ASD radiometer, and NASA's Goddard Space Flight Center's (GSFC's) field-deployable calibration artifact, the 746 Integrating Sphere Irradiance Collector (746/ISIC).[5] In March 1999 a comparison of sphere spectral radiance measurements made by these instruments revealed differences of as much as 30%.

Consequently, in September 1999 a measurement comparison was performed at the Ames SCL to resolve this discrepancy. The goals of the comparison were to evaluate the Ames measurement procedures, to validate the radiometric scale, and to establish the uncertainties assigned to the Ames 76 cm ISS and lamp–plaque over the spectral range 400–2500 nm. In addition to the Ames ASD radiometer and NASA's GSFC 746/ISIC, two instruments each from the University of Arizona's (UA's) Remote Sensing Group and the National Institute of Standards and Technology (NIST) participated in the comparison. One instrument from each facility was designed to measure the radiance in the visible to near-infrared spectral region (400–900 nm), and a second instrument was designed for operation in the shortwave infrared (1000–2500 nm).

The measurement comparison at the Ames SCL is one of a series of validation measurements overseen by NASA's EOS calibration program located within the EOS Project Science Office (PSO).[6–11] From these validation measurements, satellite, airborne, and ground-based sensors used in this long-term, global remote-sensing program are evaluated and the accuracy of their radiometric calibration is ensured. The measurement comparison at the Ames SCL confirms that calibration facilities funded by the EOS PSO, namely, the Ames SCL and NASA's GSFC Radiance Calibration Facility, are maintaining a common radiance scale and providing consistent calibrations to the EOS validation community.

Of course, the radiometric uncertainty of the calibration source is only one of a number of components in an instrument's at-sensor, in-flight uncertainty budget. One of the goals of the research reported in this paper is to reduce the uncertainty of the calibration source such that the operational uncertainties dominate the combined standard uncertainties of the measurements.

2. Sources Used in the Comparison

Three radiometric sources were measured during the comparison: the EOS–NIST Portable Radiance Source (NPR); the Ames SCL radiance source artifact, i.e., the reflectance plaque illuminated by an irradiance standard lamp; and the Ames SCL 76 cm ISS source. Each radiometric source is briefly described below.

A. EOS–NIST Portable Radiance Source

The NPR was designed to be used at NASA's EOS calibration facilities in conjunction with portable transfer radiometers to complement detector-based measurement strategies and to enhance the capabilities of the EOS calibration program. The NPR is used to validate methodologies employed at NASA facilities to calibrate sources for spectral radiance as well as to verify the spectral radiance responsivity of the transfer radiometers and instruments at the calibration facility. The NPR is a 30 cm diameter Spectralon sphere with a 10 cm diameter aperture.[12,13] The sphere is equipped with four 30 W lamps located on the sphere wall at 90° intervals about the inside of the aperture. The source was calibrated for spectral radiance over the spectral range 400–2400 nm at the primary U.S. facility for irradiance and radiance calibrations, the NIST Facility for Automated Spectroradiometric Calibrations (FASCAL).[14] Two monitor detectors mounted on the sphere wall, a silicon photodiode equipped with a photopic filter and an indium gallium arsenide (InGaAs) detector with a 20 nm bandpass filter centered at 1540 nm, are used to verify the operational stability of the source.

There are additional uncertainties associated with the operation of the source in the field. The sphere radiance with all lamps illuminated varies approximately $\pm 0.15\%$ over the central 70% of the exit port.[12] The radiometers used to measure the NPR at Ames SCL had various fields of view (FOVs) and imaged different regions of the sphere exit port. For these measurements a 0.15% uncertainty in the NPR radiance was included to account for the nonuniformity in the radiance across the NPR exit port. There is an additional uncertainty in the NPR radiance that arises from changes that may occur during shipping or during operation at the Ames SCL. The monitor signals during operation at the Ames SCL agreed with measurements at NIST made before the comparison to within 0.25%. The NPR was measured by two NIST-maintained transfer radiometers during the intercomparison, the EOS Visible Transfer Radiometer (VXR) and the EOS Short-Wave Infrared Transfer Radiometer (SWIXR), at NIST before and after shipment as well as at Ames. The VXR measurements of the sphere radiance at NIST agreed with measurements at the Ames SCL to within $\pm 0.25\%$ for all channels; the SWIXR measurements agreed to within $\pm 0.5\%$. The VXR has been involved

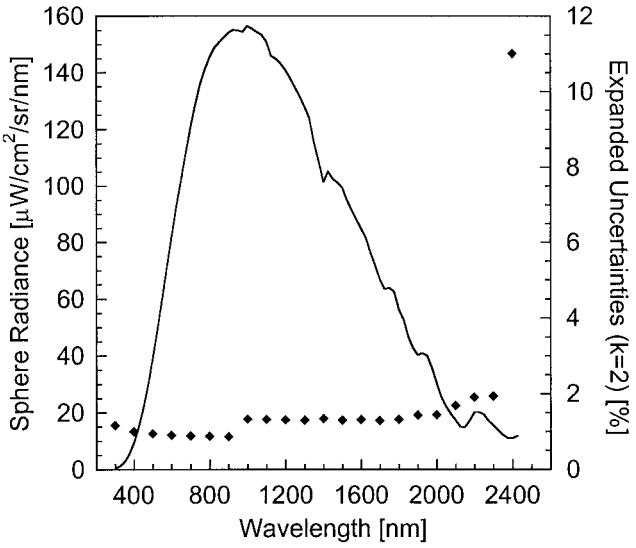

Fig. 1. NPR radiance (curve) and uncertainty (filled diamonds) from 400 to 2500 nm.

in a number of field comparisons, and its responsivity has remained constant during shipping. The SWIXR was designed to be calibrated in the field by the NPR; hence its stability during shipping had not been carefully assessed at the time of the Ames comparison. The sources of the differences in the SWIXR measurements of the NPR include possible changes in both the NPR radiance and the SWIXR responsivity. Based on results from both the monitor photodiodes and the transfer radiometers, an additional uncertainty in NPR radiance of 0.25% was included. The NPR is deployed with a known spectral radiance along with established uncertainties; the NPR radiance with the relative combined standard uncertainties used in the intercomparison is shown in Fig. 1.

B. Ames SCL Irradiance Lamp and Reflectance Plaque

The Ames SCL radiance scale is obtained with a 25 cm square commercial Spectralon diffuse reflectance plaque calibrated for 8° directional–hemispherical reflectance by a commercial laboratory and illuminated by a 1000 W irradiance standard lamp (designated F-494). The radiance from the illuminated reflectance plaque is calculated from the plaque reflectance, the irradiance of the lamp, and the distance of the lamp to the plaque. During normal operation, the plaque is illuminated by the lamp at normal incidence and the radiometer to be calibrated is positioned at an angle of 45°. To first order, the measurement equation for spectral radiance, $L(\lambda)$, is

$$L(\lambda) = f(0°/45°, \lambda)(50/r)^2 E(\lambda, 50\ \text{cm}), \qquad (1)$$

where $f(0°/45°, \lambda)$ is the bidirectional reflectance distribution function (BRDF) for this geometry, λ is the wavelength, r is the distance between the lamp and the plaque, and $E(\lambda, 50\ \text{cm})$ is the spectral irradiance of the standard lamp at 50 cm.[5] Bidirectional reflectance factor $R(0°/45°, \lambda)$ (Ref. 15) is equal to $\pi f(0°/45°, \lambda)$. Because the manufacturer of the Ames plaque provided 8° directional–hemispherical reflectance values $R(8°/\text{h}, \lambda)$, $R(8°/\text{h}, \lambda)$ is equal to $R(0°/45°, \lambda)$ if the plaque is isotropic and diffuse (i.e., a Lambertian diffuser). Under that assumption, Eq. (1) becomes

$$L(\lambda) = \frac{R(8°/\text{h}, \lambda)}{\pi}(50/r)^2 E(\lambda, 50\ \text{cm}). \qquad (2)$$

The irradiance of the Ames standard lamp was calibrated in January 1997 at a distance of 50 cm referenced to the front of the lamp mounting posts.[16] The distance used during the comparison at Ames was 0.994 m ± 0.0006 m.

In the utilization of the lamp–plaque by the Ames SCL, two corrections are applied to Eq. (2). The first arises from the assumption that $R(0°/45°, \lambda) = R(8°/\text{h}, \lambda)$, which is not strictly true because the BRDF is a function of the incident and observation angles.[17] In the calibrations described here Ames assumes $R(0°/45°, \lambda) = 1.013\, R(8°/\text{h}, \lambda)$, where the 1.013 factor is the average of the 45 reflectance factors for pressed polytetrafluoroethylene at 550 nm reported by Barnes and Hsia[18] and for fluorocarbon at 550 nm reported by Hsia and Weidner.[19] The second correction arises because the standard lamp is operated at a distance from the plaque (99.6 cm) that is greater than the calibration distance (50 cm), and the location of the radiometric center of the lamp with respect to the 50 cm calibration distance is unknown. In 1998 the deviation of three lamps from the $1/r^2$ scaling law for distances of 1 m to 1.5 m was determined to be 0.53–0.28 cm. For the Ames comparison, the offset for lamp F494 was assumed to be 0.3 cm, which is equal to one half of the diameter of the lamppost; i.e., we assume that the filament is centered with respect to the mounting structure. This gives a correction factor of $[(50 + 0.3)/(99.6 + 0.3)]^2 (100/50)^2 = 1.014$.

The uncertainty in the plaque radiance includes the uncertainty in the lamp calibration along with a number of additional uncertainties, described below. The magnitude of the lamp current affects the spectral irradiance. Following Early *et al.*,[20]

$$\frac{u_i(L)}{L} = \left(\frac{654.6\ \text{nm}}{\lambda}\right)(0.0006/\text{mA})u(I), \qquad (3)$$

where $u(I)$ is the standard uncertainty in the lamp current. The estimated uncertainty in lamp current is 1 mA, giving an uncertainty of 0.1% or less.

To estimate the uncertainty of the assumption that $R(0°/45°, \lambda) = R(8°/\text{h}, \lambda)$, we use a uniform probability-distribution function, bounded by 1.00 and 1.03, which gives a standard uncertainty of 0.0087.[21] We evaluate the uncertainty in the distance correction factor in the same manner as the reflectance correction factor, by estimating upper and lower limits to the offset and applying a uniform probability distribution. If the offset is bounded by 0.0

Table 1. Relative Standard Uncertainty Components, Expressed in Percent, That Affect Spectral Radiance $L(\lambda)$ of the Ames Plaque Independently of the Radiometer Under Consideration

	Width (nm)			
Component	400	650	950	2200
Reflectance factor correction	0.87	0.87	0.87	0.87
Correction for $1/r^2$ scaling	0.34	0.34	0.34	0.34
R (8°/h, λ)	0.57	0.53	0.51	0.51
Distance	0.12	0.12	0.12	0.12
Alignment (lamp to plaque)	0.12	0.12	0.12	0.12
E (λ, 50 cm)	0.75	0.55	0.67	1.86
Lamp current	0.10	0.06	0.04	0.02
Stray light[a]	0.01	0.06	1.02	1.45
Wavelength interpolation[b]	0.02	0.02	0.2	0.02

[a]Stray light at 400 and 650 nm calculated from VXR blocked panel data. Stray light at 950 and 2200 nm calculated from SWIXR blocked panel data and reflectance of black anodized aluminum.
[b]Wavelength interpolation uncertainty determined from MODTRAN calculation of 1 m of air at sea level.

and 0.6 cm, the relative standard uncertainty is 0.34%.

Ambient stray light is an issue for this method of obtaining radiance because of interreflections between the 1000 W lamp and the plaque or surrounding structures. For these experiments an on-axis aperture was used to restrict the illumination in the forward direction such that only the plaque was illuminated. Direct irradiation of the transfer radiometers by the lamp was prevented by inclusion of an opaque baffle, and other baffles were used to collect the off-axis flux from the lamp. In addition, an opaque disk was placed between the transfer radiometer's input aperture and the plaque in an attempt to measure any stray radiation.

Lamp spectral irradiance values are determined by use of a cubic spline interpolation of the reported NIST irradiances. This interpolation perfectly reproduces the NIST irradiance values for the lamp but also introduces an uncertainty in wavelength regions where water vapor absorbs.

Finally, there are a number of uncertainty components in the plaque measurements that depend on details of the transfer radiometer. For example, there is a component of uncertainty related to the goniometric distribution of the lamp irradiance and the geometric field of view of the particular radiometer. The target area on the plaque as viewed by the radiometers corresponds to a range of goniometric angles in pitch and yaw with respect to the lamp; these are greater than the 2° (full angle) over which the lamp was calibrated. Early *et al.*[20] give

$$\frac{u_g(L)}{L} = -0.005\,\frac{\theta}{2^\circ}, \tag{4}$$

where θ is the angle from the center of the lamp to the edge of the area viewed by the radiometer on the plaque and $u_g(L)$ is the relative standard uncertainty in spectral radiance that is due to the lamp goniometry. For the ASD radiometer at 22 cm with an 8° field of view, $\theta = 2.5°$.

Table 2. Measurement Wavelengths, Spectral Bandwidths, and Combined Standard Uncertainties ($k = 1$) of Radiance Measurements with the VXR Transfer Radiometer

Channel Number	Wavelength (nm)	Bandwidth (nm)	Uncertainty (%)
1	411.43	10.8	2.0
2	441.62	10.3	2.0
3	547.96	10.4	2.0
4	661.82	9.6	2.0
5	774.78	11.6	2.0
6	870.0	12	3.0

Other sources of uncertainty affect the radiance of the plaque as well; see Walker *et al.*,[14] App. D of Early *et al.*,[20] and Sec. 5 of Johnson *et al.*,[5] A 1.0 mm uncertainty in distance r leads to a standard uncertainty in the plaque radiance, $u_r(L)$, of 0.12%; an angular alignment uncertainty $u(\theta) = 0.2°$ also contributes 0.12% to the uncertainty budget. The major uncertainty components are listed in Table 1.

C. Ames SCL 76 cm Integrating Sphere Source

The Ames 76 cm ISS is an aluminum sphere coated on its interior surface with barium sulfate. The ISS has a 29.85 cm diameter aperture and is operated in an upward-emitting geometry. The ISS is equipped with twelve 45 W lamps operated at a nominal 6.4 V. Three power supplies are used to operate sets of four lamps. The lamps are wired in series and are operated in constant-current mode. Lamps that are shut off are replaced in the circuit by a short. Individual lamp voltages, lamp total operating times, and power supply bank currents are recorded manually. For MAS and MASTER sensor calibrations, data are taken at four lamp levels to establish the linearity of the instruments over the dynamic range of typical cloud and Earth surface scene radiances. A linear regression between digital counts and the corresponding radiance levels permits the gain to be determined for each channel as a function of digital counts. The system's responsivity is then used to generate at-sensor radiance values.

3. Radiometers Used in the Comparison

A brief description of each instrument used in the comparison, the spectral range covered (or channel center wavelength) and bandpass, the calibration protocol, and the estimated relative combined standard measurement uncertainties are provided below.

A. EOS Visible Transfer Radiometer

The VXR was designed and built by NIST for the EOS PSO at NASA's GSFC. The VXR is an improved version of the Sea-Viewing Wide Field-of-View Sensor (SeaWiFS) transfer radiometer.[22] Both instruments use a camera lens to focus the object at the field stop. Behind the field stop, six wedge-shaped mirrors with spherical curvature focus the field stop at six image

Table 3. Measurement Wavelengths, Spectral Bandwidths, and Combined Standard Uncertainties ($k = 1$) of Radiance Measurements with the UAVNIR Transfer Radiometer[a]

Channel Number	Wavelength (nm)	Bandwidth (nm)
1	412.8	15.1
2	441.8	11.9
3	488.0	9.7
4	550.3	9.9
5	666.5	9.8
6	746.9	10.7
7	868.1	14.0

[a]In all cases the uncertainty is 2.2%.

Table 4. Measurement Wavelengths, Spectral Bandwidths and Combined Standard Uncertainties ($k = 1$) of Radiance Measurements with the UASWIR Transfer Radiometer

Filter Number	Wavelength (nm)	Bandwidth (nm)	Uncertainty (%)
1	1243.5	15.2	3.3
2	1380.8	29.0	Uncalibrated
3	1646.0	23.4	3.3
4	2133.6	55.1	3.6
5	2164.3	40.8	3.6
6	2207.9	44.5	3.7
7	2263.0	49.3	3.7
8	2332.3	63.1	3.8
9	2403.2	70.3	3.9

locations, where individual interference filters and silicon photodiodes are located. The temperature of the field stop, filters, and detectors is maintained at 26 °C. An on-axis optical system is used to align and focus the VXR. The FOV of the VXR is 2.5°, and the minimum object distance is 85 cm.

The VXR was calibrated against lamp-illuminated integrating sphere sources. The band-center wavelengths, bandpasses, and relative combined standard uncertainties for the six VXR channels are given in Table 2.

B. EOS Short-Wave Infrared Transfer Radiometer

The EOS SWIXR is a scanning, double-grating monochromator-based instrument.[23] It is equipped with all-reflective input optics and a liquid-nitrogen-cooled indium antimonide (InSb) detector. The instrument has a full-angle FOV of 5.2°. A cold filter with transmittance of less than 10^{-3} is placed in front of the InSb detector to reduce stray light and thermal infrared background radiation incident upon the detector. Order-sorting filters further reduce stray light in the system. The SWIXR has a stray-light rejection of 10^{-7}, a wavelength reproducibility of 0.1 nm, and a corrected wavelength uncertainty of 0.2 nm. Chopped output from the detector is sent to a three-stage transimpedance amplifier and then to a lock-in amplifier. The instrument is calibrated with the NPR, which is calibrated for spectral radiance at the FASCAL. One determines the responsivity by simply taking the ratio of the measured signal divided by the calibrated radiance at the corrected wavelength setting of the spectroradiometer. The relative combined standard uncertainty in the SWIXR's responsivity is approximately 2% from 1000 to 2200 nm and increases slightly to 2.5% at 2400 nm.

C. University of Arizona Visible–Near-Infrared Transfer Radiometer

The UA Visible–Near-Infrared Transfer Radiometer (UAVNIR) is a seven-channel filter radiometer with a detector that employs three silicon photodiodes (p-on-n type) arranged in a light-trapping configuration.[24] It was built and independently characterized by the UA's Optical Sciences Center Remote Sensing Group. Narrowband interference filters are used for spectral selection within the seven channels. An eighth radiometer position is permanently shuttered to enable the radiometer's dark signal to be measured. To enhance stability, the temperature of the filters and detectors is maintained at 30 °C. Two precision apertures separated by a precisely measured distance fix the FOV and throughput of the radiometer.

The laboratory calibration of the UAVNIR is traceable to NIST primary standards. Radiometric calibrations were made in the laboratory by direct reference to a standard of spectral irradiance purchased from NIST (F-330) and to one obtained from a secondary-standards laboratory (F-297). The standard is a quartz halogen lamp rated at 1000 W mounted in a special bi-post base. We actively control the current by measuring it with a precision 0.01 Ω shunt and applying a voltage to the constant-current programming inputs of the dc power supplies.

In calibrating the UAVNIR radiometer we removed the front aperture of the radiometer and aligned the radiometer to the lamp axis with a distance of 1.000 m from the lamp pins to the rear aperture of the radiometer. The output of the radiometer is sampled for each band. The set of irradiance values for the lamp as supplied by NIST or by the secondary laboratory is fitted to a polynomial-corrected exponential function, which we then use in a numerical integration to find the band-averaged irradiance of the lamp in each band. The measured voltage and band-averaged irradiance determine a calibration coefficient. This irradiance calibration was converted into a radiance calibration of the radiometer by use of the measured aperture diameters and their known separation. The estimated relative combined standard uncertainty in this calibration is 2.2% and is slightly wavelength dependent.

We checked the radiance calibration of the radiometer by illuminating a Spectralon panel with lamp F-297 at a distance of 50 cm. The BRDF of the panel was measured before the experiment. The radiance of the panel was calculated by use of the lamp irradiance and the BRDF. The band-averaged radiance in each band was calculated by the same method as above, and a radiance calibration was determined.

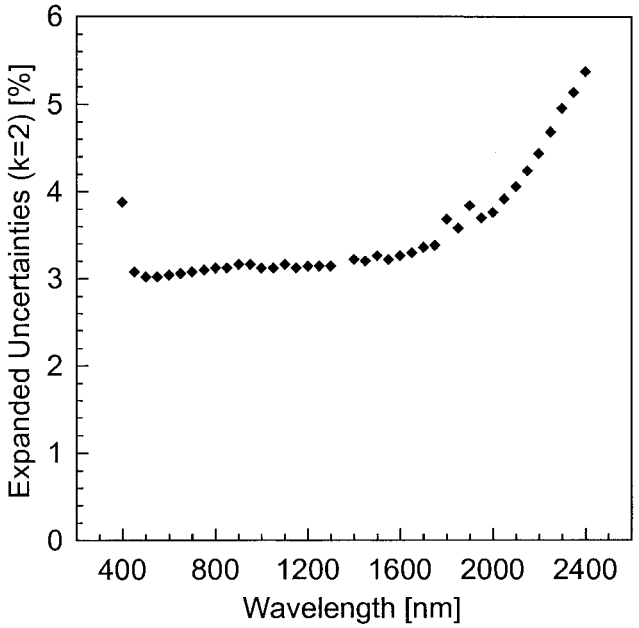

Fig. 2. Combined standard uncertainty in the spectral responsivity of the 746/ISIC.

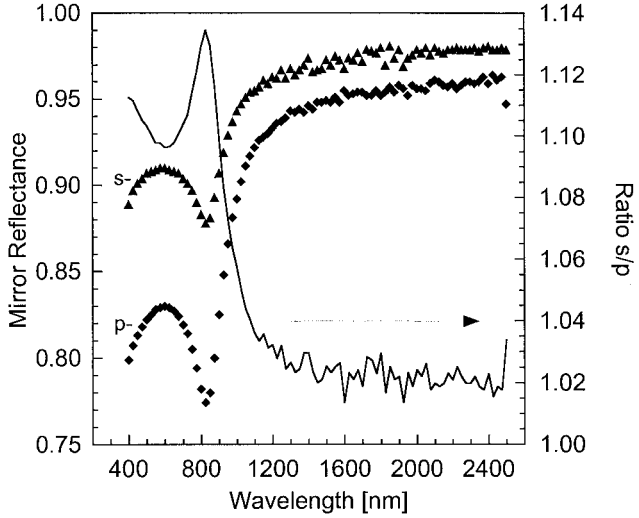

Fig. 3. Mirror reflectance for *s*- and *p*-polarized light at 45° incidence and reflectance. The ratio of the *s* and *p* reflectance (solid curve) is also shown.

The average difference between the two laboratory calibrations was 0.51%, with a standard deviation of 0.43%.

Finally, outside the laboratory in Tucson, the radiometer was calibrated to the Sun. An atmospherically attenuated direct solar beam was used to illuminate a Spectralon panel, which was viewed along the normal by the radiometer. The diffuse field contribution was determined by blocking the direct beam and correcting for the small portion of the diffuse field that was also blocked. Using exoatmospheric solar irradiance values, the solar calibration gave results that agreed with the laboratory calibrations to within 0.5% for four bands and with a difference of less than 2.1% for all bands. Band-center wavelengths, spectral bandpasses, and relative combined standard uncertainties for the UAVNIR radiometer are given in Table 3.

D. University of Arizona ShortWave InfraRed Transfer Radiometer

The UASWIR is a 12 channel filter radiometer incorporating an InSb photodiode as its detector. Three channels have band-center wavelengths below 1 μm: at 746.9, 868.9, and 940.0 nm, with bandpasses of 10.5, 12.1, and 16.2 nm, respectively. Nine channels have center wavelengths beyond 1 μm: filter band centers, bandpasses, and calibration uncertainties are listed in Table 4. Similarly to those of the UAVNIR instrument, the UASWIR channels were chosen to have center wavelengths to correspond to those in the MODIS and the ASTER. As with the UAVNIR, a pair of precision apertures separated by a known distance determines the SWIR radiometer's throughput. Light incident upon the radiometer is chopped, and the detector's output is sent to a lock-in amplifier. To reduce noise and increase sensitivity, the InSb detector is operated at liquid-nitrogen temperature (77 K), along with the apertures, baffles, and amplifier. To further reduce unwanted thermal infrared background signal, a cold filter, also at liquid-nitrogen temperature, is used to block radiation at wavelengths longer than 2.7 μm.

The UASWIR is calibrated for spectral radiance responsivity by use of a standard irradiance lamp and a diffusely reflecting Spectralon panel. The lamp and panel are the same as those used in the calibration of the UAVNIR instrument. For the UASWIR, the panel is placed 2.33 m from the standard lamp to provide calibration radiances for the radiometer that approximate the typical on-orbit radiances for the MODIS and ASTER instruments. The relative combined standard uncertainty for the instrument is estimated to be 3.3% to 3.9%.[25]

E. NASA's GSFC 746–Integrating Sphere Irradiance Collector

NASA's GSFC maintains and operates an Optronic Laboratories Model 746 scanning single-grating monochromator-based spectroradiometer equipped with a 10.2 cm diameter integrating sphere irradiance collector (ISIC) located at the monochromator's entrance port.[4] In the visible–near-infrared wavelength region from 400 to 1000 nm the 746–ISIC collects data in 10 nm steps, with an instrument bandwidth of 10 nm. In the shortwave-infrared spectral region from 1000 to 1600 nm, data are obtained every 20 nm with a bandwidth of 20 nm. In the wavelength region from 1600 to 2400 nm, data are obtained every 20 nm with a 40 nm bandwidth. A silicon detector is used for the 400–1000 nm spectral range; while a lead sulfide detector is used for the 1000–2400 nm spectral range.

The 746–ISIC transfers the irradiance calibration from a NIST-calibrated irradiance standard lamp to

Table 5. Determination of Fold Mirror Reflectance and Radiometer Polarization Sensitivities at Ames on 1 September 1999

Wavelength (nm)	NIST STARR Reflectance[a]	VXR Reflectance	Reflectance Ratio	0°/60° Radiance Ratio
VXR				
411.77	0.848	0.844	0.996	1.0044
441.01	0.856	0.855	0.999	1.0043
548.4	0.868	0.869	1.001	0.9986
661.4	0.867	0.867	1.001	1.0015
775.47	0.842	0.846	1.004	1.0075
869.97	0.843	0.840	0.996	0.9945
UAVNIR				
412.78	0.848	0.844	0.996	1.0000
441.79	0.856	0.852	0.996	1.0001
488.03	0.863	0.861	0.998	1.0003
550.29	0.869	0.869	1.000	1.0007
666.55	0.866	0.866	1.000	1.0007
746.91	0.852	0.852	1.000	1.0001
868.07	0.841	0.840	0.999	1.0000
UASWIR				
746.9	0.852	0.856	1.004	
868.7	0.842	0.843	1.001	
940.0	0.896	0.894	0.998	
1243.5	0.951	0.950	0.999	
1380.8	0.957	0.950	0.993	
1646.0	0.963	0.964	1.001	
2133.5	0.968	0.972	1.004	
2164.2	0.968	0.969	1.001	
2207.8	0.969	0.969	1.000	
2262.9	0.969	0.969	1.000	
2332.2	0.969	0.971	1.002	
2402.9	0.970	0.972	1.002	

[a]Reflectance calculated as the average of the mirror s and p reflectances measured at the STARR facility.

the integrating sphere being measured.[26] The 746–ISIC is calibrated for irradiance responsivity. To determine the radiance of the sphere under test, one must know the area of the sphere's exit port as well as the distance between the sphere's exit port and the ISIC's entrance port. The sphere's radiance is then calculated from the irradiance responsivity of the 746–ISIC according to the following equation:

$$L(\lambda) = E_{\text{Sphere}}(\lambda)\frac{Z^2}{A_{\text{Sphere}}} = \frac{S_{\text{Lamp}}(\lambda)}{S_{\text{Sphere}}(\lambda)}E_{\text{Lamp}}(\lambda)\frac{(d^2 + r_1^2 + r_2^2)}{A_{\text{Sphere}}}, \quad (5)$$

where $S_{\text{Lamp}}(\lambda)$ and $S_{\text{Sphere}}(\lambda)$ are the measured signals from the lamp and the sphere, respectively, at wavelength λ; Z is the view factor; A_{Sphere} is the area of the integrating sphere's exit port; $E_{\text{Lamp}}(\lambda)$ is the spectral irradiance of the standard lamp; d is the distance between the 746–ISIC's entrance aperture and the integrating sphere's exit port aperture; and r_1 and r_2 are the radii of the integrating sphere's exit port and the 746–ISIC's irradiance collector aperture.

Instrumental uncertainties that arise from stray light, wavelength uncertainty, random noise, and lock-in detector phase angle contribute to the overall uncertainty budget. There are additional uncertainties in measuring the radiance of an integrating sphere source that arise from the distance between the 746–ISIC's entrance aperture and the integrating sphere source's exit port, from the sphere's exit port area, and from the fact that the 746/ISIC measured the radiance from the entire exit port, which contributes to higher overall uncertainty because of edge effects and nonuniformity in the sphere's radiance over the exit port. The 746–ISIC's combined standard uncertainties are shown in Fig. 2 as a function of wavelength.

F. NASA's Ames SCL Analytical Spectral Device's FieldSpec Radiometer

The ASD FieldSpec FR portable spectroradiometer utilizes hand-held input optics coupled to the spectrometer through a fiber bundle. The radiometer has three grating spectrometers and associated detectors that enable measurements to be made over a wavelength range from 350 to 2500 nm. The first spectrometer uses a 512 element, silicon photodiode array with a fixed grating and is designed for the wavelength range from 350 to 1000 nm. The second spec-

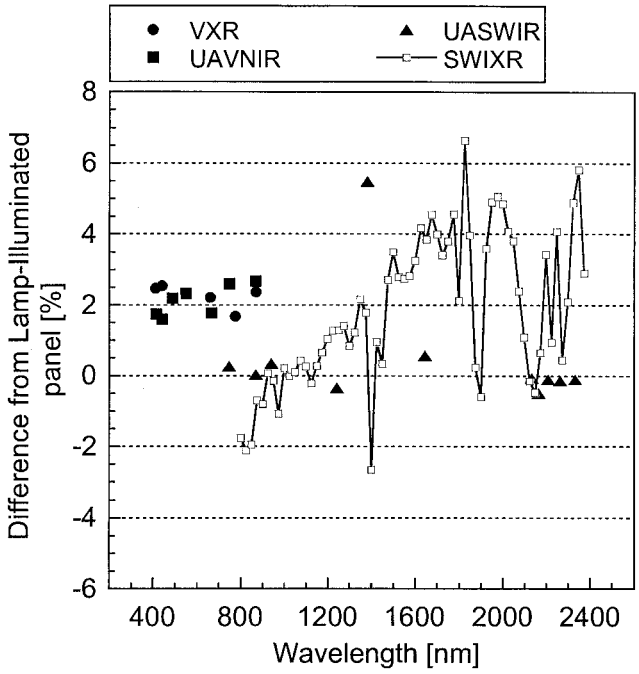

Fig. 4. Results of radiance measurements of the lamp-illuminated panel.

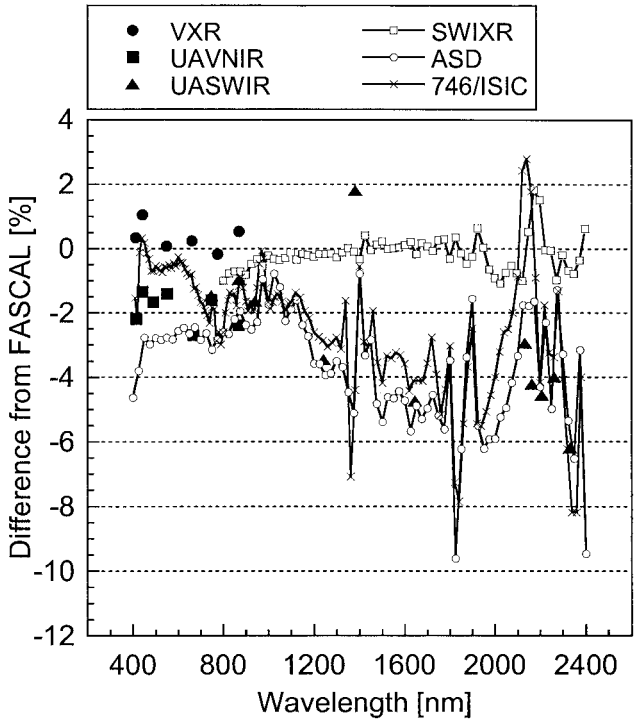

Fig. 5. Percent difference between measured and calibrated radiance of the NPR source.

trometer, designed for the wavelength range from 900 to 1850 nm, uses a scanned grating and a single-element, thermoelectrically cooled indium gallium arsenide (InGaAs) detector. The final spectrometer element also uses a scanned grating configuration with a thermoelectrically cooled InGaAs detector for the wavelength range from 1700 to 2500 nm. The instrument has a spectral resolution of approximately 3 nm at 700 nm, of 10 nm at 1500 nm, and of 10 nm at 2100 nm. Evaluation of the uncertainties of the scale transfer from the lamp-illuminated plaque to the Ames 76 cm ISS was one of the primary goals of the comparison.

4. Comparison of Band-Averaged Spectral Radiances

The VXR, UAVNIR, and UASWIR transfer instruments made radiance measurements of the NPR, the Ames lamp–plaque, and the Ames ISS, using filters with different center wavelengths and spectral responses. To compare measurements made by these radiometers, we computed band-averaged spectral radiances for each source according to the following equation:

$$L_c(i, j) = \frac{\int_{\lambda_1}^{\lambda_2} L_{\mathrm{ref}}(\lambda) R(i, j, \lambda) \mathrm{d}\lambda}{\int_{\lambda_1}^{\lambda_2} R(i, j, \lambda) \mathrm{d}\lambda}. \quad (6)$$

In Eq. (6), $L_c(i, j)$ is the computed band-averaged spectral radiance for band j of radiometer i, $L_{\mathrm{ref}}(\lambda)$ is the reference spectral radiance at wavelength λ, $R(i, j, \lambda)$ is the relative spectral response of radiometer i, band j, and λ_1 and λ_2 and are the lower and upper wavelength limits, respectively; of the integration. $L_{\mathrm{ref}}(\lambda)$ for the comparison of radiometer measurements of the NPR was the spectral radiance measured at the FASCAL before the Ames comparison. $L_{\mathrm{ref}}(\lambda)$ for the lamp–plaque was the Ames spectral radiance calculated by use of the calibrated irradiances for lamp FEL F494 and the 8° directional–hemispherical reflectance-derived BRDF of the panel. $L_{\mathrm{ref}}(\lambda)$ for the ISS was the spectral radiance measured by the Ames ASD radiometer. The calculated band-averaged radiances were compared to the radiometer-measured band-averaged radiances for the three sources according to the following equation:

$$P(i, j) = 100 \frac{L_m(i, j) - L_c(i, j)}{L_c(i, j)}, \quad (7)$$

where $P(i, j)$ is the percent difference of each radiometer measurement $L_m(i, j)$ from the computed band-averaged spectral radiance $L_c(i, j)$.

5. Polarization Issues in the Measurement of the Ames 76 cm Integrating Sphere Source

Measuring the spectral radiance of the Ames ISS presented the comparison participants with an interesting radiometric challenge. The ISS is operated in an upward-emitting geometry, whereas many of the transfer radiometers are either constrained to operate horizontally or have not been characterized for vertical operation. For example, the SWIXR and

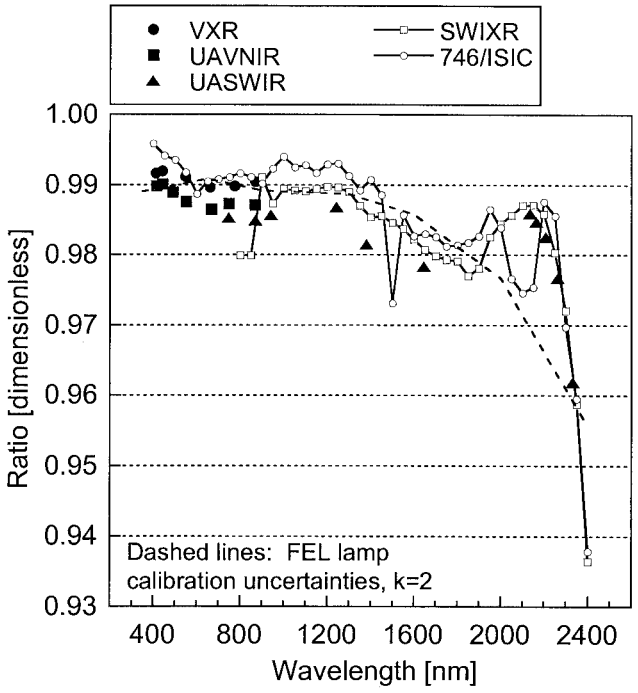

Fig. 6. Results of the comparison of two FEL lamps: lamp F496 calibrated against the 1990 NIST irradiance scale and lamp F512 calibrated against the 2000 NIST irradiance scale. The ratio $S(F512)/E(512)$ to $S(F496)/E(496)$ is plotted versus wavelength for each radiometer, where S is the radiometer signal and E is the NIST-reported lamp irradiance.

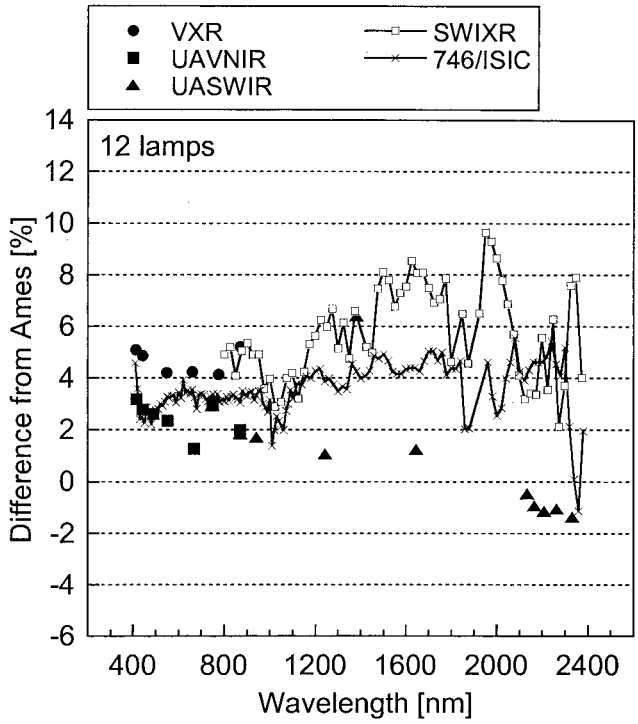

Fig. 7. Percent difference between the Ames ASD-measured ISS radiance (12 lamps on) and the radiance measured by the other radiometers.

UASWIR instruments are constrained to operate horizontally owing to their large size and their use of liquid-nitrogen-cooled detectors. The VXR and UAVNIR, although they are able to measure in a vertical configuration, were not characterized before the comparison for vertical operation. For the 746–ISIC and Ames ASD radiometer; vertical operation is not an issue. One can rotate the integrating sphere attached to the entrance slit of the 746–ISIC monochromator in a vertical plane to view upward-emitting sources. The fiber optic coupling of the Ames ASD radiometer's input optic to the spectrometer enables the input optic to be positioned for viewing the upward-emitting ISS.

To address this problem, a 45° incident–45° reflecting fold mirror was employed to enable horizontally operating radiometers to measure the Ames ISS. However, the introduction of this fold mirror above the integrating sphere not only slightly decreased the detected light by an amount equal to the mirror's reflectance but also introduced an increased horizontal polarization component to the measured light. To quantify this effect, we measured the mirror's polarized reflectance. The mirror's reflectance was measured at the NIST Spectral Trifunction Automated Reference Reflectometer (STARR) facility[27] for *s*- and *p*-polarized light at 45° incidence and −45° degrees from 400 to 2500 nm. The STARR reflectance measurements of the mirror are shown in Fig. 3.

To measure the spectral radiance of the ISS by using the fold mirror, we determined the effective mirror reflectance and the polarization dependence of the spectral responsivities of the VXR, UAVNIR, SWIXR, and UASWIR in the following manner: we assumed that the output of the NPR is unpolarized. The radiometers viewed the NPR directly and with the fold mirror deployed at its 45° incidence/45° reflectance geometry. In the visible–near-infrared wavelength region, the effective mirror reflectance calculated from VXR and UAVNIR data obtained with and without the mirror deviated ±0.4% from the NIST STARR measurements. In the shortwave-infrared wavelength region, the UASWIR radiometer deviated −0.2% to +0.4% from the NIST values. These results indicated that the mirror reflectance had not changed from the time of the NIST STARR measurements to the time of deployment at Ames. We determined the polarization dependence of the spectral responsivity of the VXR by measuring the NPR with the mirror, rotating the VXR 60°, and remeasuring the NPR with the mirror. Ideally, we should have the VXR rotated 90° to determine its polarization sensitivity. However, to do so requires a special mount, which was not available for the Ames comparison. Likewise, the UAVNIR viewed the NPR with the mirror at orientations of 0° and 90° rotated. The results of the VXR and UAVNIR measurements are shown in Table 5 and indicate that the polarization sensitivities of these radiometers are quite small. As mentioned above, the UASWIR polarization sensitivity was unable to be directly determined because of an inability to operate in a rotated geometry. How-

ever, the on-axis design of the UASWIR, similar to that of the UAVNIR, and the excellent agreement between the UASWIR- and the NIST STARR-measured mirror effective reflectance also listed in Table 5 led to the assumption that the polarization sensitivity of the UASWIR was negligible.

The use of two gratings in the SWIXR gives that radiometer a strong polarization dependence in its spectral responsivity. We determined the SWIXR's polarization response by measuring the NPR source with and without the mirror in place. The derivation of the equations used to correct the SWIXR radiance measurements for polarization effects is provided in Appendix A. Because the SWIXR was constrained to operate in a horizontal geometry, the use of the fold mirror for measurements of the radiance of the Ames ISS caused an additional uncertainty of approximately 4% in the SWIXR measurements. This increased uncertainty can be attributed to mirror alignment issues as well as to the instrument's significant polarization dependence.

6. Results and Discussion

The measurement comparison at NASA's Ames SCL was held from 31 August to 2 September 1999. The goals of the comparison were to evaluate the Ames SCL measurement protocols, to validate the Ames ISS radiance as determined and maintained by use of the ASD instrument as a transfer radiometer, and to quantify uncertainties in the calibration of the ISS and the Ames lamp–plaque.

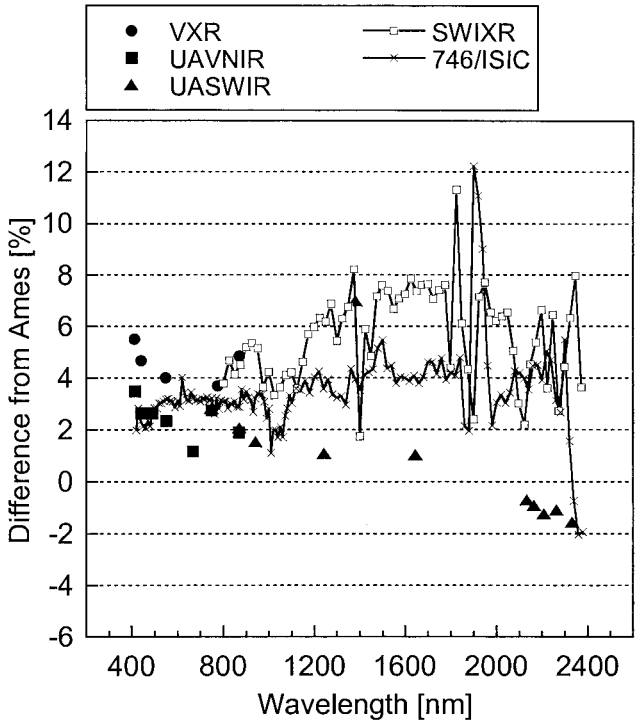

Fig. 8. Percent difference between the Ames ASD-measured ISS radiance (nine lamps on) and the radiance measured by the other radiometers.

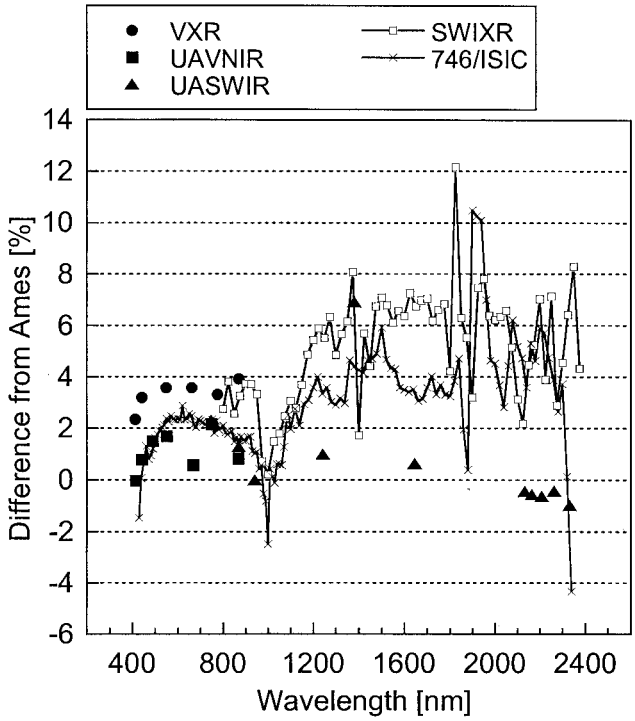

Fig. 9. Percent difference between the Ames ASD-measured ISS radiance (six lamps on) and the radiance measured by the other radiometers.

A. Lamp-Illuminated Ames Plaque

Before the start of the intercomparison, the setup and procedures developed at the Ames SCL for measurement of its lamp-illuminated plaque using its transfer instrument, the ASD radiometer were examined. Several significant sources of systematic error were identified. First, the Ames protocols assumed that the standard irradiance lamps were used at a distance of 100 cm from the reflectance plaque. The distance from the irradiance lamp to the reflectance plaque was measured to be 99.6 cm instead of the assumed 100.0 cm. Second, a baffle was installed between the lamp and the reflectance plaque. The baffle was slightly undersized, causing vignetting of the irradiance from the lamp to the plaque. Third, the ASD radiometer was not properly aligned to permit viewing of the center of the reflectance plaque. Fourth, the plaque reflectance was not actually measured. Instead, representative values of the 8° hemispherical reflectance of the plaque divided by π were used. Fifth, black cloth was used in close proximity to the lamp–reflectance plaque setup to control stray light; the cloth had low reflectance in the visible and the near infrared but as much as 38% reflectance in the SWIR, resulting in significant calibration errors from stray light. Each of these factors contributed to an overall error in the radiance scale produced at the Ames SCL. This error was then propagated through to determination of the ISS radiance. Before the comparison was begun, recommendations were made to improve the overall measurement technique and to eliminate or reduce these sources of error.

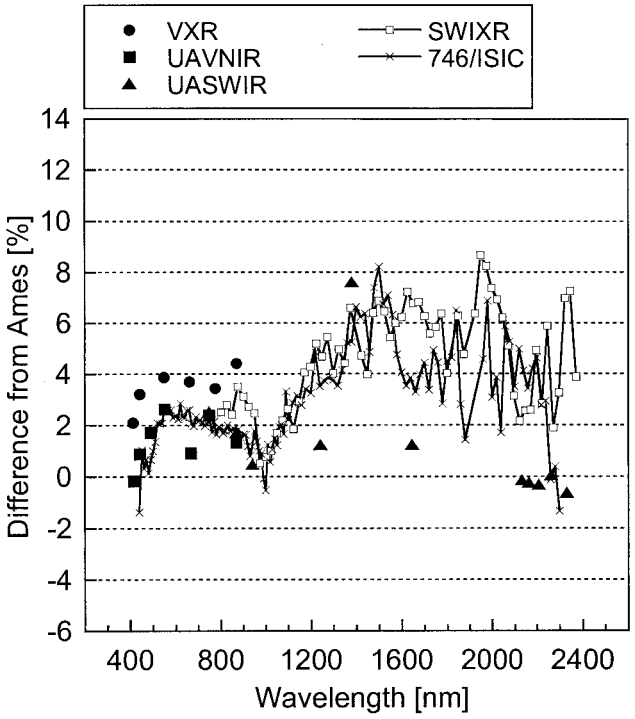

Fig. 10. Percent difference between the Ames ASD-measured ISS radiance (three lamps on) and the radiance measured by the other radiometers.

The Ames irradiance standard lamp-illuminated Spectralon plaque was measured by the comparison participants on 1 September. The results of comparing these measurements are shown in Fig. 4. As described in Section 4 of this paper, the spectral radiance of the plaque was calculated from Eq. (2) with the correction factors for $1/r^2$ and reflectance distribution applied. This spectral radiance was then compared with the radiances measured by the VXR, UAVNIR, SWIXR, and UASWIR radiometers. The plaque was illuminated by Ames's 1000 W FEL lamp F494 with a 13 January 1997 irradiance calibration date, and plaque BRDF values were calculated by use of the Ames prescription from values of the 8° directional–hemispherical reflectance. The 746/ISIC was not able to measure the plaque radiance because of geometrical constraints imposed by its input cosine collector (e.g., no defining aperture). The plaque is used to calibrate the Ames ASD radiometer, so that instrument was precluded from participating in the measurements. With the exception of measurements made in the water vapor absorption region near 1385 nm, the measurements made by the NIST and UA radiometers all agreed to within their combined measurement uncertainties. The VXR and the UAVNIR measurements of the illuminated plaque show excellent agreement and are approximately 2% higher than the Ames-predicted radiance. The UASWIR instrument measured the illuminated plaque twice, and the average of those measurements is plotted in the figure. The UASWIR-instrument-measured radiance showed excellent agreement with the Ames predicted radiance over the entire spectral range, with the exception of the 1385 nm channel. The SWIXR-measured radiance was 2% lower than the Ames-calculated radiance below 1000 nm, increasing to approximately 4% higher than the calculated radiance at 1800 nm and oscillating within that range from 2000 to 2400 nm. Whereas the measurements of the UASWIR and the SWIXR agreed to within their combined measurement uncertainties, the SWIXR measurements in the 1600 nm water vapor window region appear to be 3–4% higher than those of the UASWIR instrument. Both the UASWIR- and the SWIXR-measured radiances were 2–4% lower than the VXR- and UAVNIR-measured radiances in their overlap wavelength region below 1000 nm. These differences, although they are within the combined measurement uncertainties of the radiometers, could be due to differences in radiometer alignment and FOV coupled with spatial nonuniformities in the plaque reflectance and in its illumination.

From the lamp–plaque results shown in Fig. 4, the radiance scale used by the Ames ASD radiometer in measurements of integrating sphere sources appears to be approximately 2% lower than the NIST scale from 400 to 1000 nm and 0–6% lower than the NIST scale from 1000 to 2400 nm. This finding is significant

Table 6. Short Term (i.e., Day-to-Day) Repeatability of the Ames 76 cm Diameter Integrating Sphere Operated at the Nine-Lamp Illumination Level on 1 and 2 September

Wavelength (nm)	Nine-Lamp Level Measurement Difference
VXR	
411.77	0.033
441.01	0.259
548.4	0.175
661.4	0.277
775.47	0.239
869.97	0.260
UAVNIR	
412.78	0.022
441.79	0.084
488.03	0.074
550.29	0.090
666.55	0.069
746.91	0.092
868.07	0.097
UASWIR	
746.95	−0.141
868.68	−0.684
1243.53	−0.376
1380.82	−1.115
1646.05	0.061
2133.48	0.098
2164.17	−0.400
2207.75	−0.396
2262.76	−0.536
2332.17	−0.296

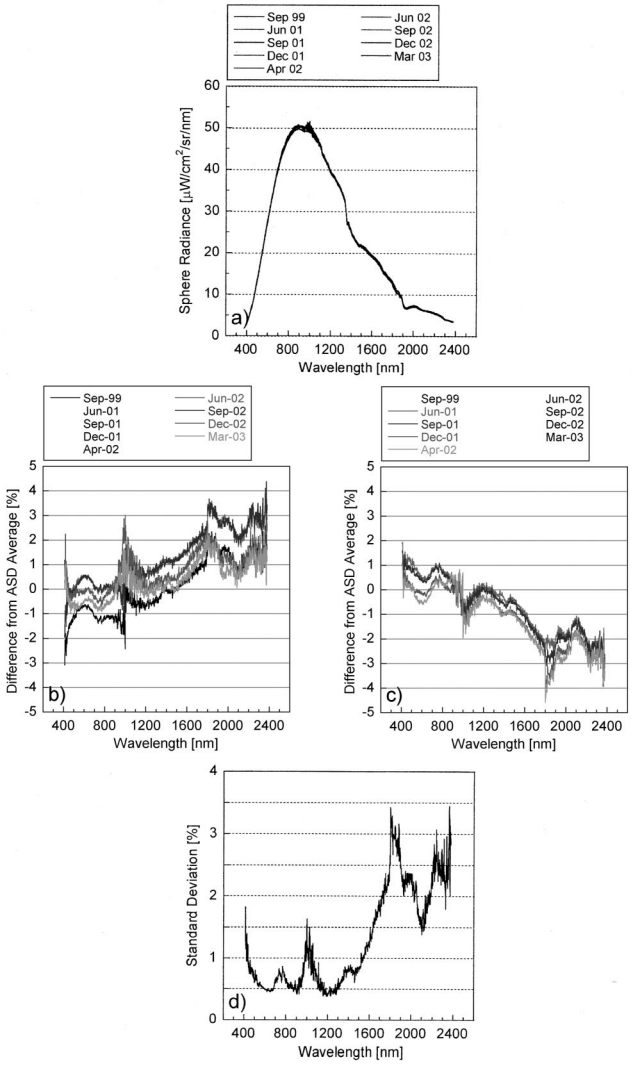

Fig. 11. Percent difference from the average of Ames ASD radiance measurements of the Ames ISS at the twelve-lamp illumination level. The ASD measurements were acquired on nine dates from September 1999 to March 2003. The percent standard deviation from the average is also shown.

in that the ability of the Ames SCL to make accurate radiance measurements of integrating spheres critically depends on its ability to obtain, transfer, and maintain an accurate radiance scale by using its lamp–plaque as a source and its ASD radiometer as a transfer instrument. According to Fig. 4, these differences of at least 2% below 1000 nm and 6% at certain wavelengths above 1000 nm will be propagated through the Ames integrating sphere measurements. These differences represent a significant fraction of, or are equal to, the target sphere radiance uncertainties of 3% in the visible and 6% in the shortwave infrared.

B. Measurements of the NPR

The NPR was measured by the comparison participants on 31 August. Results of NPR radiance measurements are shown in Fig. 5. The NPR radiance determined by the NIST radiometers agreed with the predicted values to within 1.0%. This is not surprising in that the NPR, used as a calibration source for the SWIXR, and the Optronics Laboratory 420 integrating sphere source, used as a calibration source for the VXR, were both calibrated at the FASCAL. However, such good agreement gave confidence in the stability of both the radiometers and the NPR during the intercomparison.

In the visible spectral region from 400 to 1000 nm, the VXR, the UAVNIR, and the 746/ISIC and Ames ASD radiometers measured the NPR four-lamp level radiance with a mean difference between its measured radiances and the NIST calibration of 2% and a variance among the instruments of approximately 3%. The UAVNIR instrument measured radiance approximately 2% lower than expected, within its measurement uncertainty and consistent with previous measurement comparisons with the VXR.[5,9] The 746/ISIC-measured radiance also agreed with the NIST-calibrated radiance to within 2%, while the Ames ASD radiometer-measured radiance was approximately 2–4% lower than the FASCAL-measured value, consistent with the direction of the differences seen in the lamp–plaque comparison of Fig. 4.

In the SWIR spectral region from 1000 to 2400 nm, excluding the water vapor absorption regions near 1385 and 1850 nm, the UASWIR and the 746/ISIC and Ames ASD radiometers all showed a similar trend. These instruments measured radiances 2% lower than expected at 1000 nm, decreasing to 4% lower than expected at 1500 nm and remaining 4–6% lower than expected from 1500 to 2100 nm. In the 746/ISIC the difference increased to approximately 2.5% at 2100 nm, returning to −4% from 2200 nm to 2400 nm, in agreement with the UASWIR and Ames ASD values.

Although the percent differences shown in Fig. 5 are within the combined measurement uncertainties of the radiometers, the UAVNIR, UASWIR, 746/ISIC, and Ames ASD radiometer measurements in the shortwave infrared demonstrate internal consistency but disagree with the NPR values that were assigned by the FASCAL. Moreover, comparisons of the UASWIR and Ames ASD results with those of the SWIXR show trends similar to those seen in measurements of the Ames lamp–plaque. Differences between the NPR measurements made by various radiometers could arise from the different calibration approaches adopted by the measuring institutions. The UAVNIR, the UASWIR, and the Ames ASD radiometer rely on irradiance standard lamps and reflectance panels to derive their radiance respon sivities. The 746/ISIC also relies on an irradiance standard lamp to transfer an irradiance scale to the sphere being measured and on aperture sizes and distance to subsequently calculate radiance. The calibrations of the NIST VXR and SWIXR are radiance based and use an Optronics Laboratory 420 integrating sphere and the NPR, respectively, both of which are calibrated by the FASCAL.

The irradiance scale maintained at the NIST

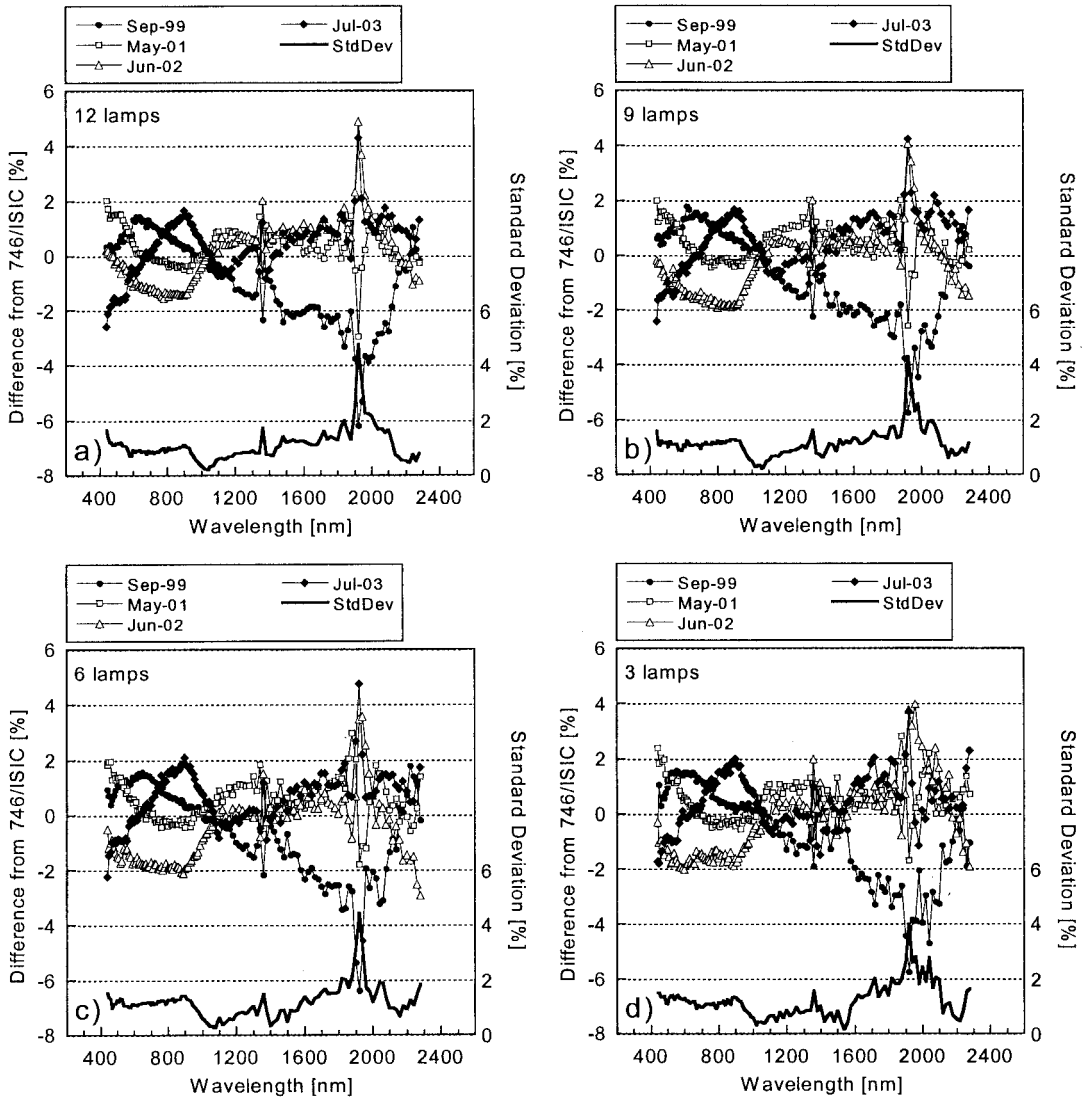

Fig. 12. Percent difference from the average of 746/ISIC radiance measurements of the Ames ISS at the lamp illumination levels shown. The 746/ISIC measurements were acquired on four dates from September 1999 to July 2003. The percent standard deviation from the average is also shown for each of the four illumination levels.

was recently rederived by use of detector-based standards.[28] This rederived scale is called the NIST 2000 irradiance scale. The total expanded uncertainties of the detector-based spectral irradiance scale are reduced relative to the source-based scale by factor of 2 from 250 to 900 nm and by as much as a factor of 10 from 900 to 2400 nm. In April 2001 a comparison of two FEL standard lamps was made at NASA's GSFC: lamp F496 was calibrated against the 1990 NIST irradiance scale and lamp F512 was calibrated against the 2000 irradiance scale.[7] At the time of this comparison, lamps F496 and F512 had been operated a total of 2.5 and 3 h, respectively. The VXR, SWIXR, UA-VNIR, UASWIR, and 746/ISIC measured the radiance from a NIST Spectralon plaque illuminated at a distance of 1 m by the two irradiance standard lamps. Figure 6 presents the result of that comparison, showing differences of approximately 1% in the visible, 2% from 1000 to 2000 nm, and as much as 6% at 2400 nm. These results agree with those reported by Yoon *et al.*[28] in their comparison of the difference in detector-based and source-based spectral irradiances of three working standard lamps. The spectral dependence, magnitude, and direction of the differences between the 1990 and 2000 NIST irradiance scales mimic the differences in radiance measurements of the NPR by the irradiance-lamp- and radiance-sphere-calibrated radiometers. Based on these results, recalibration of the irradiance standard lamps used by the UA, the GSFC, and the SCL should significantly improve the agreement of their radiance measurements with the NIST radiometers and greatly reduce the uncertainty in those measurements.

C. Measurements of the Ames 76 cm Diameter Integrating Sphere Source

The Ames ISS was measured by the 746/ISIC on 31 August and by the other radiometers on 1 and

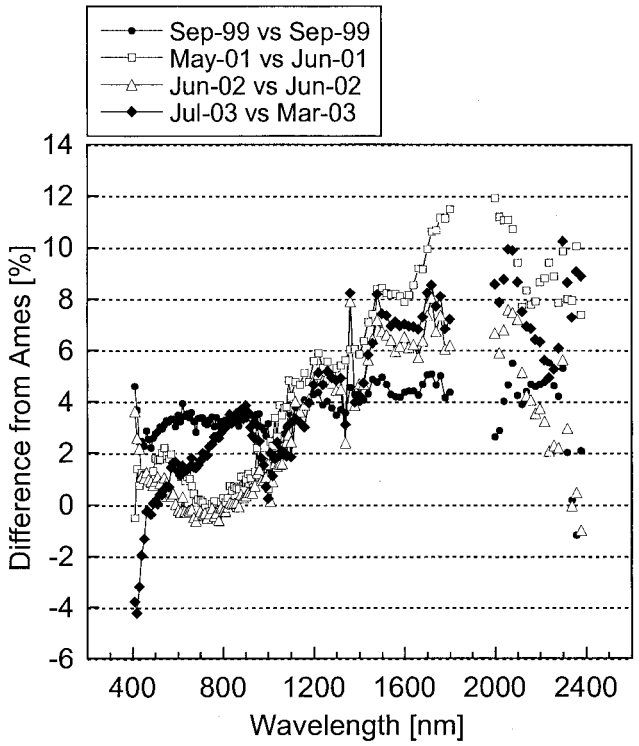

Fig. 13. Percent difference of the four chronologically closest radiance measurements of the Ames ISS by the 746/ISIC and the SCL ASD radiometer from September 1999 to July 2003. The first dates listed are the dates of the 746/ISIC measurements.

2 September. The sphere was operated in an upward-looking geometry. The Ames ASD and the 746/ISIC measured the sphere radiance in this geometry, whereas the UA and NIST–EOS transfer radiometers measured the radiance in a horizontal geometry, using a flat mirror at an angle of 45° to image a portion of the sphere's exit port. The flat mirror was placed on a rotation stage and rotated such that light from the sphere was reflected off the mirror and into the radiometers. As discussed in Section 5 of this paper, the mirror slightly polarized the beam, and alignment was difficult, resulting in higher uncertainties in the measurement of sphere radiance with the transfer radiometers. The Ames ISS was measured at the twelve-lamp, nine-lamp, six-, and three-lamp illumination levels. The sphere radiance scaled with the number of lamps illuminated to within 1% as measured by the VXR and UASWIR instruments.

Results of comparing the difference between the Ames ASD-radiometer-measured sphere radiances and those measured by the other radiometers are shown in Figs. 7–10 for the four sphere radiance levels. Measuring the ISS source with 12 lamps illuminated and disregarding the water vapor absorption regions near 1385 and 1850 nm yielded VXR, UAVNIR, and 746/ISIC measurements that were within their combined measurement uncertainties and showed agreement similar to that seen for measurements of the NPR. The UAVNIR and the 746/ISIC showed good agreement and were approximately 2% lower than the VXR measurements. The Ames ASD-determined radiances in this wavelength region were 1.28–5.09% lower than the ensemble of transfer radiometer measurements.

In the near-infrared and shortwave-infrared spectral regions, the SWIXR, the UASWIR, and the 746/ISIC also showed difference trends similar to those seen in measurements of the NPR. The UASWIR measurements showed good agreement with those of the ASD radiometer, with differences from −1.37% to 3.38% across the spectral range from 747 to 2332 nm. The 746/ISIC and SWIXR radiances were consistently higher than the Ames ASD radiances. The 746/ISIC radiances were 1.39% higher at 1010 nm and increased to 4.5% higher from 1400 to 2400 nm. The SWIXR measured the ISS initially with 15 nm and then 5 nm bandpasses on 1 September. The 15 nm bandpass SWIXR measurements shown in Fig. 7 were 3.97% higher at 1000 nm, increasing to approximately 8.34% higher from 1400 to 2000 nm and oscillating in the range from 2.13% to 7.91% higher from 2000 to 2400 nm. The 5 nm bandpass SWIXR measurements were systematically 2% higher than the 15 nm bandpass measurements at all wavelengths. Despite the fact that this difference is within the measurement uncertainty of the SWIXR, a problem in reproducibly setting the SWIXR slit widths was discovered following the Ames deployment. This problem arises when the SWIXR slits are driven from a wide-open position (e.g., 15 nm) to a narrower position (e.g., 5 nm). This was the source of part of the nonreproducibility in the SWIXR measurements at the two slit widths and has led to the current SWIXR protocol of first homing the slits before adjusting the slits from wide to narrow configurations. Finally, the NIST and UA radiometers showed excellent agreement in their respective near-infrared overlap regions.

Measurements of the ISS with nine, six, and three lamps illuminated gave similar results for the VXR, the UAVNIR, the 746/ISIC, and the UASWIR instruments relative to the Ames ASD radiometer. In the visible spectral region the VXR measurements were 3.71% to 5.51% higher than the Ames-determined radiances for nine lamps and 2.10% to 4.42% higher for six and three lamps. The UAVNIR measurements again were consistently 2% to 3% lower than the VXR measurements for these lamp levels and showed good agreement with measurements made by the 746/ISIC. The UASWIR measured radiances were again in good agreement with the Ames ASD radiances; they were 0.62% lower to 2.52% higher from 747 to 2332 nm, if the 1380 nm water vapor region is disregarded. The 746/ISIC and the SWIXR radiances agreed to within 3% over the spectral range from 1000 to 2400 nm and were consistently 2% to 6% higher than those determined by the Ames ASD instrument.

The VXR, UAVNIR, SWIXR, and UASWIR radiometers measured the 76 cm diameter sphere nine-lamp illumination level on 1 and 2 September. We analyzed these data to obtain information on the

short-time repeatability of the sphere. Table 6 presents the percent differences between the nine-lamp level radiometer measurements on the two days. During the comparison, the ISS showed day-to-day stability of better than 0.26% and 0.68% below and above 1000 nm, respectively.

In summary, Ames ISS radiances measured by the Ames ASD radiometer were approximately 2.5% to 5% lower than those measured by the NIST VXR and 2.5% to 7% lower than those measured by the NIST SWIXR. These results are consistent with the comparisons performed by use of the Ames lamp–plaque and the NPR. The UAVNIR-radiometer-measured radiances are 1% to 2% lower than the NIST VXR measurements. The UASWIR-radiometer-measured radiances are 2% to 7% lower than those measured by the NIST SWIXR and agree closely with the SCL ASD measurements. The 746/ISIC radiances are 1% to 2% lower than the NIST VXR measurements and agree closely with the UAVNIR measurements. The 746/ISIC radiances in the shortwave infrared agree within −1% to 7% with the NIST SWIXR measurements. In general, the radiance measurement uncertainties of the UA, GSFC, and Ames SCL radiometers were reduced and radiance measurement agreement improved through the recalibration of their irradiance lamps against the NIST 2000 detector-based irradiance scale.

D. Long-Term Comparison and Stability of Radiance Measurements of the 76 cm Diameter Integrating Sphere Source

From March 1999 to July 2003 the Ames SCL operated its 76 cm diameter ISS with the same set of lamps. From September 1999 to March 2003, Ames measured the twelve-lamp radiance of the sphere nine times, using its ASD radiometer. The percent difference of each of these measurements from the average and the standard deviation of these measurements are shown in Fig. 11. In this figure, ASD radiometer measurements acquired in June 2001, September 2001, December 2001, and April 2002 show sphere radiances higher than the average below 1000 nm and lower than the average above 1000 nm. ASD measurements made on the other five dates show an opposite trend. One possible explanation for this behavior could be an increase in the sphere color temperature for the four measurements from June 2001 to April 2002. A close examination of the ASD-radiometer-measured radiances in the region of the sphere radiance maxima for the two groups of measurements showed no discernable wavelength shift, which indicates that a sphere color temperature change was probably not the source of the difference. A second possible explanation could be the presence of some unknown internal operation or optimization process within the ASD used to match its visible–near-infrared and shortwave-infrared spectra; conclusive proof that this is the source of the difference would require detailed knowledge of the ASD radiometer and is not addressed in this paper.

The data of Fig. 11 can also be used to determine the long-term repeatability of the Ames ISS. If we ignore the spectral regions where data from the various spectrometers within the instrument are merged, e.g., the region near 1000 nm and the region near 1800 nm, the percent standard deviation of the nine measurements in the visible–near-infrared wavelength region was 1.82% at 410 nm, decreasing to 0.43% at 907 nm. Similarly, the percent standard deviation of the nine measurements in the shortwave-infrared wavelength region was 0.39% at 1200 nm, increasing to 3.14% at 2372 nm. According to these ASD measurements, the ISS showed very good long-term radiance repeatability from September 1999 to March 2003.

In addition to the comparison series of experiments, the 746/ISIC made a series of validation measurements of the 76 cm diameter ISS radiance. On four occasions from September 1999 to July 2003, the GSFC 746/ISIC measured the twelve-, nine-, six-, and three-lamp radiance of the ISS. The percent difference and the standard deviation of these measurements from the average for wavelengths from 440 to 2300 nm are shown in Fig. 12. In these figures, the percent difference of the September 1999 measurements peaks in the vicinity of 620 nm, steadily declines to a minimum in the vicinity of 1920 nm, and then rises toward 2400 nm. The percent difference of the 746/ISIC measurements made in May 2001, June 2002, and July 2003 are relatively flat through the near-infrared and shortwave-infrared wavelength regions. A significant part of the difference in these data can be attributed to GSFC's use of irradiance standard calibration lamps calibrated against the 1990–1992 and 2000 NIST irradiance scales. In the September 1999 measurements, an irradiance lamp calibrated against the 1990 NIST scale was used. For dates after September 1999, irradiance standard lamps calibrated against the 2000 NIST irradiance scale were used.

If we ignore the water vapor absorption regions from 1350 to 1500 nm and from 1800 to 2000 nm, the 746/ISIC data in Fig. 12 support the ASD instrument's data of Fig. 11, showing very good long-term sphere radiance repeatability. The standard deviations from the averages shown in Figs. 12(a)–12(d) are less than 1.90% below 1000 nm and less than 2.13% above 1000 nm.

A comparison of the chronologically closest ISS 12 lamp level measurements made by the Ames ASD and the GSFC 746/ISIC is shown in Fig. 13. The ASD and 746/ISIC instruments differed by −4.22% to 4.60% in the visible–near-infrared wavelength region and by −1.18% to 11.92% in the shortwave-infrared wavelength region. The ASD and 746/ISIC differences in September 1999 show significantly less variation with wavelength than the post-September 1999 differences. In September 1999 the 746/ISIC and ASD radiometers were both calibrated by use of a NIST irradiance standard lamp calibrated against the 1990–1992 NIST irradiance scale. For those comparisons after September 1999, the 746/ISIC was

calibrated by use of lamps calibrated against the 2000 scale. The shapes of the differences between the 746/ISIC and the ASD radiometer for dates after September 1999 are characteristic of the wavelength-dependent differences in the two NIST irradiance scales. It appears from these data that Ames used irradiance lamps calibrated against the 1990 NIST scale from the time of the Ames radiometric measurement campaign in September 1999 to March 2003.

7. Conclusions

In March 1999, large differences in the 76 cm sphere radiance between the 746/ISIC and the Ames ASD radiometer were reported, motivating a measurement comparison involving those instruments as well as instruments from the UA and the NIST. Before the measurement comparison in September 1999, a number of specific recommendations were made to improve the overall Ames SCL measurement protocol. These recommendations were implemented and significantly reduced the measurement uncertainties at the facility. During the measurement comparison in September 1999, NPR measurements with the five transfer radiometers and the Ames ASD radiometer agreed to within approximately 2% in the visible and 4% in the SWIR relative to the average. The variance in measurements of the Ames 76 cm ISS was slightly larger, primarily because of the repeatability of measurements made using the fold mirror. In this case the measurements agreed to within approximately 4% in the visible and 8% in the SWIR. When these uncertainties are combined with the target uncertainties of 3% in the visible and 6% in the shortwave infrared, the results demonstrate that the uncertainty in the radiance of the Ames 76 cm ISS determined by use of the Ames SCL protocols and transfer radiometer is slightly within the target uncertainties required for MAS and MASTER instruments when they are used in the vicarious calibration of satellite instruments.

Using the NPR as a field calibration source demonstrated that, with further refinement, including recalibration of the Ames SCL irradiance standard lamps, the Ames ASD measurement uncertainties could be reduced by a factor of 2 to the 1–2% level in the visible and to 2–4% in the SWIR. Based on the results of this comparison, recalibration of the Ames SCL, GSFC, and UA irradiance standard lamps followed by their use in radiometer calibrations not only would greatly reduce their calibration uncertainties but also would improve their agreement with the NIST radiometers.

There are additional sphere-related uncertainties associated with the calibration of airborne remote-sensing instruments. Sphere stability and repeatability are two important uncertainty components in the use of spheres for predeployment and postdeployment calibrations of these instruments. Sphere repeatability was determined from the Ames radiometric measurement comparison. The short-term (i.e., day-to-day) repeatability of the 76 cm diameter ISS as determined from VXR, UAVNIR, and UASWIR measurements of the nine-lamp illumination level was −0.68% to 0.26%.

The measurement comparison in September 1999 validated the SCL's radiometric scale at that time. Scale maintenance is a critical component of a sensor calibration facility. To establish the Ames SCL's ability to maintain its radiometric scales we determined the long-term (i.e., multiyear) repeatability of the 76 cm ISS sphere radiance from Ames ASD radiometric measurements of the twelve-lamp illumination level and from 746/ISIC measurements of the twelve-, nine-, six-, and three-lamp levels; the repeatability was 0.39% to −3.14%.

In summary, the measurement comparison in September 1999 and subsequent timely measurements with the 746/ISIC validated the Ames SCL's radiance scale and uncertainties over the time frame from September 1999 through July 2003. Recalibration of their standard irradiance lamps was recommended to reduce the uncertainty in their radiance scales by a factor of 2 in both the visible and the shortwave-infrared regions.

Appendix A

A degree of polarization was introduced by the use of a fold mirror in the radiance measurements of the Ames 76 cm diameter ISS. Because of its double-monochromator-based design, the SWIXR has a strongly polarization-dependent spectral responsivity. We used measurements of the NPR with and without the fold mirror to determine the polarization dependence of the SWIXR's spectral responsivity. The derivation of the equations used to correct for this dependence are provided below.

The general measurement equation for any radiometer can be written as follows:

$$S(\lambda) = \int_{\lambda_1}^{\lambda_2} R(\lambda) L(\lambda) \mathrm{d}\lambda. \tag{A1}$$

In Eq. (A1), $S(\lambda)$ is the radiometer signal as a function of wavelength λ, $R(\lambda)$ is the radiometer's relative spectral responsivity, $L(\lambda)$ is the spectral radiance of the source being measured, and λ_1 and λ_2 are the wavelength limits of the integration. In a polarization-sensitive instrument such as the SWIXR, Eq. (A1) can be rewritten as

$$S(\lambda) = \int_{\lambda_1}^{\lambda_2} [R_s(\lambda) L_s(\lambda) + R_p(\lambda) L_p] \mathrm{d}\lambda, \tag{A2}$$

where $R_s(\lambda)$ and $R_p(\lambda)$ are the radiometer responsivities to s- and p-polarized light and $L_s(\lambda)$ and $L_p(\lambda)$ are the separated s- and p-polarized radiance of the source, respectively. The unpolarized radiant output of the source, $L(\lambda)$, is equal to the sum of the s- and p-polarized components. That is,

$$L(\lambda) = L_s(\lambda) + L_p(\lambda), \tag{A3}$$

where $L(\lambda)$ was measured before the Ames comparison at the NIST FASCAL.

Neglecting band averaging for the sake of simplification yields

$$S(\lambda) = R_s(\lambda)L_s(\lambda) + R_p(\lambda)L_p(\lambda). \quad \text{(A4)}$$

The assumption is made that the output of the NPR is unpolarized. Then

$$L_s(\lambda) = L_p(\lambda) = \frac{L(\lambda)}{2}, \quad \text{(A5)}$$

which, substituted for $L_s(\lambda)$ and $L_p(\lambda)$ in Eq. (A4), gives

$$S(\lambda) = \frac{[R_s(\lambda) + R_p(\lambda)]\, L(\lambda)}{2}. \quad \text{(A6)}$$

Introducing a mirror between the SWIXR and the integrating sphere leads to the following equation:

$$S(\lambda) = [R_s(\lambda)r_s(\lambda)L_s(\lambda) + R_p(\lambda)r_p(\lambda)L_p(\lambda)], \quad \text{(A7)}$$

where $r_s(\lambda)$ and $r_p(\lambda)$ are the s- and p-polarized reflectances of the mirror, respectively, measured before the Ames comparison in the NIST STARR facility.

When the SWIXR is calibrated by direct viewing of the NPR, the SWIXR signal is compared to the FASCAL-measured radiance of NPR according to the following equation:

$$S(\lambda) = R(\lambda)L(\lambda). \quad \text{(A8)}$$

The measured responsivity of the SWIXR, $R(\lambda)$, can be related to the s- and p-polarized SWIXR responsivities by

$$R(\lambda) = \frac{[R_s(\lambda) + R_p(\lambda)]}{2}. \quad \text{(A9)}$$

Eliminating the λ for purposes of simplification yields the following ratio of the SWIXR measurements of NPR with and without the mirror:

$$\frac{S^M}{S} = \frac{R_s r_s L_s + R_p r_p L_p}{R_s L_s + R_p L_p} = \frac{R_s r_s + R_p r_p}{R_s + R_p}, \quad \text{(A10)}$$

where S^M is the SWIXR signal measured with the mirror. Using Eq. (A9), we can rewrite Eq. (A10) as

$$\frac{S^M}{S} = \frac{R_s r_s + R_p r_p}{2R} = \frac{R_s r_s + (2R - R_s) r_p}{2R} \quad \text{(A11)}$$

and solving for R_S leads to

$$R_s = 2R\left(\frac{S^M}{S} - r_p\right) \Big/ r_s - r_p\,. \quad \text{(A12)}$$

Similarly for R_p:

$$R_p = 2R\left(1 - \frac{S^M / S^{-r_p}}{r_s - r_p}\right). \quad \text{(A13)}$$

In Eqs. (A12) and (A13), R_s and R_p are expressed in terms of measured quantities.

For SWIXR measurements of the Ames 76 cm diameter ISS, the signal, S^A, can be expressed as follows:

$$S^A = R_s r_s L_s{}^A + R_p r_p L_p{}^A, \quad \text{(A14)}$$

where, similarly to the NPR,

$$L_s{}^A(\lambda) = L_p{}^A(\lambda) = \frac{L^A(\lambda)}{2}. \quad \text{(A15)}$$

Using Eqs. (A14) and (A15), we can express the signal from the 76 cm diameter ISS as

$$S^A = \left(\frac{R_s r_s + R_p r_p}{2}\right) L^A. \quad \text{(A16)}$$

Equation (A16) can be solved for L^A to give

$$L^A = S^A \left(\frac{R_s r_s + R_p r_p}{2}\right)^{-1}. \quad \text{(A17)}$$

Equation (A17) for L^A with inputs for R_s and R_p from Eqs. (A12) and (A13) is valid if the orientation of the fold mirror with respect to the SWIXR is identical in measurements of the NPR and the ISS. Because the ISS is calibrated and used in an upward-emitting configuration and the NPR is operated in a horizontal-emitting configuration, it was necessary to rotate the fold mirror 90° for the measurements on the two sources, which introduced a coordinate rotation to Eq. (A17) in which $r_s \Rightarrow r_p$ and $r_p \Rightarrow r_s$ and resulted in Eq. (A18) below. Equation (A18) was used to account for the polarization dependence of the SWIXR responsivity and to determine the unpolarized radiance of the ISS:

$$L^A = S^A \left(\frac{R_s r_p + R_p r_s}{2}\right)^{-1}. \quad \text{(A18)}$$

The authors thank the following members of the NIST Optical Technology Division for their support in this research: Edward A. Early for his polarized reflectance measurements of the fold mirror and Charles Gibson for his radiance calibrations of the NPR at the FASCAL. This research was supported by NASA's EOS PSO.

References and Notes

1. M. D. King, W. P. Menzel, P. S. Grant, J. S. Myers, G. T. Arnold, S. E. Platnick, L. E. Gumley, S. C. Tsay, C. C. Moeller, M. Fitzgerald, K. S. Brown, and F. G. Osterwisch, "Airborne scanning spectrometer for remote sensing of cloud density, aerosol, water vapor, and surface properties," J. Atmos. Ocean. Technol. **13,** 777–794 (1996).
2. S. Hook, J. J. Meyers, K. J. Thome, M. Fitzgerald, and A. B. Kahle, "The MODIS/ASTER Airborne Simulator (MASTER) — a new instrument for Earth science studies," Remote Sen. Environ. **76,** 93–102 (2001).
3. G. T. Arnold, M. F. Fitzgerald, P. S. Grant, S. E. Platnick, S. Tsay, J. S. Myers, M. D. King, R. O. Green, and L. Remer, "MODIS Airborne Simulator radiometric calibration," in *Earth Observing Systems,* W. L. Barnes, ed., Proc. SPIE **2820,** 56–66 (1996).
4. Certain commercial equipment, instruments, or materials are identified in this paper to foster understanding. Such identification does not imply recommendation or endorsement by the National Institute of Standards and Technology, nor does it imply that the materials or equipment identified are the best available for the purpose.
5. B. C. Johnson, S. S. Bruce, J. M. Houston, T. R. O'Brian, A. Thompson, S. B. Hooker, and J. L. Mueller, in *The Fourth SeaWiFS Intercalibration Round-Robin Experiment (SIRREX-4),* NASA Tech. Memo. 104566, S. B. Hooker and E. R. Firestone, eds. (NASA Goddard Space Flight Center, 1996), Vol. 37, pp. 1–65.
6. J. J. Butler, B. L. Markham, B. C. Johnson, S. W. Brown, H. W. Yoon, R. A. Barnes, S. F. Biggar, E. F. Zalewski, P. R. Spyak, F. Sakuma, and J. W. Cooper, "Radiometric measurement comparisons using transfer radiometers in support of the calibration of NASA's Earth Observing System (EOS) sensors," in *Sensors, Systems and Next-Generation Satellites III,* H. Fujisada, ed., Proc. SPIE **3870,** 180–192 (1999).
7. J. J. Butler, B. C. Johnson, and R. A. Barnes, "Radiometric measurement comparisons at NASA's Goddard Space Flight Center. I. The GSFC sphere sources," Earth Observer **14**(3), 3–8 (2002).
8. J. J. Butler, B. C. Johnson, and R. A. Barnes, "Radiometric measurement comparisons at NASA's Goddard Space Flight Center. II. Irradiance lamp comparisons and the NIST sphere source," Earth Observer **14**(4), 25–29 (2002).
9. J. J. Butler, S. W. Brown, R. D. Saunders, B. C. Johnson, S. F. Biggar, E. F. Zalewski, B. L. Markham, P. N. Gracey, J. B. Young, and R. A. Barnes, "Radiometric measurement comparison on the integrating sphere source used in the calibration of the Moderate Resolution Imaging Spectroradiometer (MODIS) and the Landsat 7 Enhanced Thematic Mapper Plus (ETM+)," J. Res. Natl. Inst. Stand. Technol. **108,** 199–228 (2003).
10. J. J. Butler and R. A. Barnes, "The use of transfer radiometers in validating the visible to shortwave infrared calibrations of radiance sources used by instruments in NASA's Earth Observing System," Metrologia **40,** S70–S77 (2003).
11. S. W. Brown, B. C. Johnson, H. W. Yoon, J. J. Butler, R. A. Barnes, S. F. Biggar, P. R. Spyak, K. Thome, E. Zalewski, M. Helmlinger, C. Bruegge, S. Schiller, G. Fedosejevs, R. Gauthier, S. Tsuchida, and S. Machida, "Radiometric characterization of field radiometers in support of the 1997 Lunar Lake, Nevada, experiment to determine surface reflectance and top-of-atmosphere radiance," Remote Sens. Environ. **77,** 367–376 (2001).
12. S. W. Brown and B. C. Johnson, "A portable integrating sphere source for the Earth Observing System's calibration validation programme," Int. J. Remote Sens. **24,** 215–224 (2003).
13. S. W. Brown and B. C. Johnson, "A portable integrating sphere source for radiometric calibrations from the visible to the shortwave infrared," Earth Observer **11,** 14–18 (1999).
14. J. H. Walker, R. D. Saunders, and A. T. Hattenburg, *Spectral Radiance Calibrations,* NBS Spec. Pub. 250-1 (U. S. Government Printing Office, 1987).
15. The reflectance factor is the ratio of the reflected flux to that from an ideal surface.
16. J. H. Walker, R. D. Saunders, J. K. Jackson, and D. A. McSparron, *Spectral Irradiance Calibrations,* NBS Spec. Pub. 250-20 (U. S. Government Printing Office, 1987).
17. E. A. Early, P. Y. Barnes, B. C. Johnson, J. J. Butler, C. J. Bruegge, S. F. Biggar, P. R. Spyak, and M. M. Pavlov, "Bidirectional reflectance round-robin in support of the Earth Observing System program," J. Atmos. Oceanic Technol. **17,** 1077–1091 (2000).
18. P. Y. Barnes and J. J. Hsia, *45°/0° Reflectance Factors of Pressed Polytetrafluoroethylene (PTFE) Powder,* NIST Tech. Note 1413 (U. S. Government Printing Office, 1995).
19. J. J. Hsia and V. R. Weidner, "NBS 45°/normal reflectometer for absolute reflectance factors," Metrologia **17,** 97–102 (1981).
20. E. A. Early A. Thompson, C. Johnson, J. DeLuisi, P. Disterhoft, D. Wardle, E. Wu, W. Mou, Y. Sun, T. Lucas, T. Mestechkina, L. Harrison, J. Berndt, and D. S. Hayes, "The 1995 North American interagency intercomparison of ultraviolet monitoring spectroradiometers," J. Res. Natl. Inst. Stand. Technol. **103,** 15–62 (1998).
21. B. N. Taylor and C. E. Kuyatt, *Guidelines for Evaluating and Expressing the Uncertainty of NIST Measurements Results,* NIST Tech. Note 1297 (U. S. Government Printing Office, 1994).
22. B. C. Johnson, J. B. Fowler, and C. L. Cromer, *The Sea WiFS Transfer Radiometer (SXR),* NASA Tech Memo. 1998-206892, S. B. Hooker and E. R. Firestone, eds. (NASA Goddard Space Flight Center, 1998), Vol. 1, pp. 1–58.
23. S. W. Brown, B. C. Johnson, and H. W. Yoon, "Description of a portable spectroradiometer to validate EOS radiance scales in the shortwave infrared," Earth Observer **10,** 43–47 (1998).
24. S. F. Biggar and P. N. Slater, "Preflight cross-calibration radiometers for EOS AM-1 platform visible and near-IR sources," in *Sensor Systems for the Early Earth Observing System Platforms,* W. L. Barnes, ed., Proc. SPIE **1939,** 243–249 (1993).
25. P. R. Spyak, D. S. Smith, J. Thiry, and C. Burkhart, "Shortwave infrared transfer radiometer for the calibration of the Moderate-Resolution Imaging Spectrometer and the Advance Spaceborne Thermal Emission and Reflection Radiometer," Appl. Opt. **39,** 5694–5706 (2000).
26. J. H. Walker, C. L. Cromer, and J. T. McLean, "A technique for improving the calibration of large-area sphere sources," in *Calibration of Passive Remote Observing Optical and Microwave Instrumentation,* B. W. Guenther, ed., Proc. SPIE **1493,** 224–230 (1991).
27. J. E. Proctor and P. Y. Barnes, "NIST high accuracy reference reflectometer–spectrophotometer," J. Res. Natl. Inst. Stand. Technol. **101,** 619–627 (1996).
28. H. W. Yoon, C. E. Gibson, and P. Y. Barnes, "The realization of the National Institute of Standards and Technology detector-based spectral irradiance scale," Appl. Opt. **41,** 5879–5890 (2002).